Research Article

Journal of Molecular Recognition

Received: 16 February 2010, Revised: 5 April 2010, Accepted: 22 May 2010, Published online in Wiley Online Library: 25 August 2010

(wileyonlinelibrary.com) DOI:10.1002/jmr.1063

Disruption of shape complementarity in the ribosomal protein L1–RNA contact region does not hinder specific recognition of the RNA target site

Olga Kostareva[a,b], Svetlana Tishchenko[a], Ekaterina Nikonova[a], Vladislav Kljashtorny[a], Natalia Nevskaya[a], Alexei Nikulin[a], Anna Sycheva[c], Sergei Moshkovskii[c], Wolfgang Piendl[b], Maria Garber[a] and Stanislav Nikonov[a]*

The formation of a specific and stable complex between two (macro)molecules implies complementary contact surface regions. We used ribosomal protein L1, which specifically binds a target site on 23S rRNA, to study the influence of surface modifications on the protein–RNA affinity. The threonine residue in the universally conserved triad Thr–Met–Gly significant for RNA recognition and binding was substituted by phenylalanine, valine and alanine, respectively. The crystal structure of the mutant Thr217Val of the isolated domain I of L1 from *Thermus thermophilus* (TthL1) was determined. This structure and that of two other mutants, which had been determined earlier, were analysed and compared with the structure of the wild type L1 proteins. The influence of structural changes in the mutant L1 proteins on their affinity for the specific 23S rRNA fragment was tested by kinetic experiments using surface plasmon resonance (SPR) biosensor analysis. Association rate constants undergo minor changes, whereas dissociation rate constants displayed significantly higher values in comparison with that for the wild type protein. The analysed L1 mutants recognize the specific RNA target site, but the mutant L1–23S rRNA complexes are less stable compared to the wild type complexes. Copyright © 2010 John Wiley & Sons, Ltd.

Keywords: binding kinetics; surface plasmon resonance (SPR); RNA–protein recognition; crystal structure

INTRODUCTION

Ribosomal protein L1 has a dual function as a ribosomal protein binding 23S rRNA and as a translational repressor binding its own mRNA. Bacterial and archaeal L1 proteins have been shown to be functionally interchangeable in the ribosome and in the repression of translation (Hanner *et al*., 1994). Crystal structures at atomic resolution have been determined for the isolated L1 proteins from the bacterium *Thermus thermophilus* (TthL1) (Nikonov *et al*., 1996) and from the archaea *Methanococcus jannaschii* (MjaL1) and *Methanococcus thermolithotrophicus* (MthL1) (Nevskaya *et al*., 2000, 2002) and for the L1 complexes with a specific 23S rRNA fragment (Nikulin *et al*., 2003) and with its mRNA fragment (Nevskaya *et al*., 2005, 2006; Tishchenko *et al*., 2006). Thus, L1 is a very suitable object to study how modifications in the contact surface region of the protein influence its affinity to RNA.

Protein L1 consists of two domains connected by a flexible hinge. Both domains retain their conformations in all determined L1 structures, whereas the mutual orientations of the domains can be dramatically different, corresponding to an 'open' or 'closed' conformation of the molecule. Within the TthL1–mRNA complex only domain I (TthL1d1) tightly contacts RNA (Nevskaya *et al*., 2006). Isolated TthL1d1 forms stable complexes with both rRNA and mRNA. The conformation of the isolated TthL1d1 (Figure 1A) was almost identical to that of this domain within the intact TthL1 (Tishchenko *et al*., 2007). Moreover, the structure of TthL1d1 in complex with a specific mRNA fragment showed that the protein–RNA interface is similar to that in the complex of intact TthL1 with mRNA (Tishchenko *et al*., 2008). Noteworthy, the protein–RNA interface retains an almost identical structure in all archaeal and bacterial L1–RNA complexes (Nevskaya *et al*., 2005; Tishchenko *et al*., 2006). This high degree of conservation of the L1 structure allows modelling complexes with RNA for L1 mutants from different organisms to understand how modifications of the protein relief influence its affinity for RNA.

* *Correspondence to: S. Nikonov, Institute of Protein Research, Russian Academy of Sciences, Pushchino 142290, Moscow, Russia.*
E-mail: nikonov@vega.protres.ru

a *O. Kostareva, S. Tishchenko, E. Nikonova, V. Kljashtorny, N. Nevskaya, A. Nikulin, M. Garber, S. Nikonov*
Institute of Protein Research, Russian Academy of Sciences, Pushchino 142290, Moscow, Russia

b *O. Kostareva, W. Piendl*
Biocenter, Division of Medical Biochemistry, Innsbruck Medical University, Fritz-Pregl-Str. 3, Innsbruck 6020, Austria

c *A. Sycheva, S. Moshkovskii*
Orekhovich Institute of Biomedical Chemistry, Russian Academy of Medical Sciences, Moscow, Russia

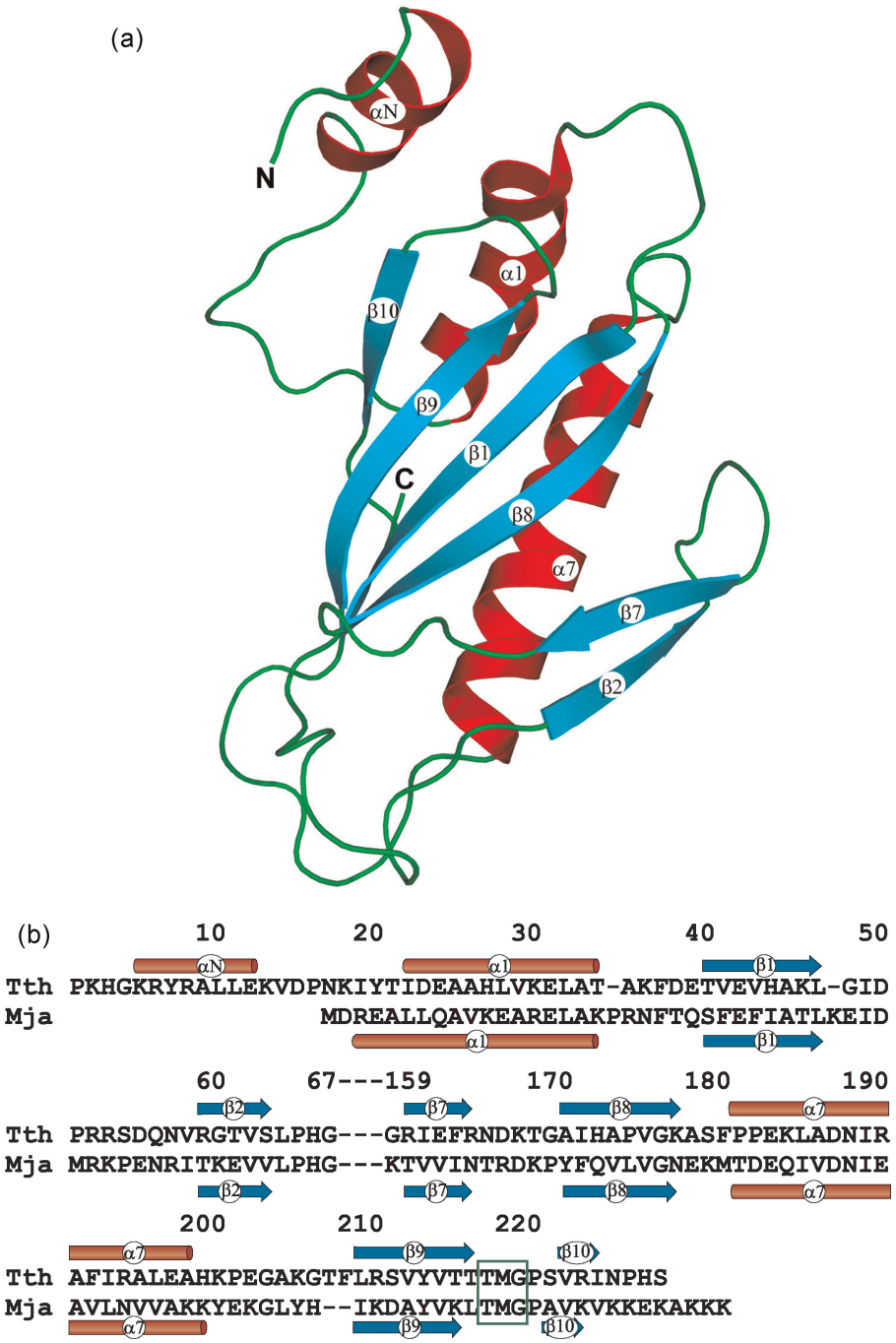

Figure 1. Spatial structure and sequence of the isolated domain I of TthL1. Numbering of residues, α-helices and β-strands corresponds to that of the entire protein. α-helices are shown in red, β-strands in blue. (A) Schematic representation of the TthL1d1 structure. (B) Alignment of the TthL1 and MjaL1 amino acid sequences (only domain I is shown). The conserved triad TMG is framed.

Comparison of the structures of the L1–RNA complexes enabled us to define the TthL1d1 surface regions responsible for RNA recognition and to select amino acid residues for point mutations. The universally conserved triad Thr–Met–Gly (residues 217–219 in TthL1; Figure 1B) plays a crucial role in the interactions of the protein with RNA and, therefore, this region seems to be most suitable to study the influence of relief modification on the RNA-binding properties of L1. Modifications were designed to create a bulge or a cavity in this region, or retain the relief unchanged. To this end, Thr217 was replaced by phenylalanine, alanine and valine, respectively. Crystal structures of Thr204Phe MjaL1 (Thr204 corresponds to Thr217 in TthL1; see Figure 1B) and of Thr217Ala TthL1 have been described earlier (Nikonova *et al.*, 2007). Here we report the crystal structure of Thr217Val TthL1d1 and the kinetic parameters of the complex formation between these L1 mutants and the specific 23S rRNA target site measured using surface plasmon resonance (SPR) biosensor analysis (Katsamba *et al.*, 2002), which allows an estimation of the apparent association (k_{ass}) and dissociation (k_{diss}) rate constants. To reveal special structural features

responsible for changes in association and dissociation of complexes formed by different L1 mutants with the 23S rRNA target site, we tried to 'reconcile' the kinetic binding data with the crystal structures of the L1 mutants.

Our results demonstrate that the point mutations on the protein surface, even a 'neutral' one such as a Thr/Ala substitution can result in an allosteric effect on the structure of neighbouring regions and an appearance of surface bulges. Deteriorations of surface complementarity had a weak effect on the RNA–protein recognition but dramatically impaired life time of the protein–RNA complexes.

MATERIALS AND METHODS

Plasmid construction

Amino acid substitution Thr217Val was introduced into the isolated domain I of TthL1 by an overlap extension PCR-based site-directed mutagenesis method (Ho *et al*., 1989). As PCR templates, we used pET11a-PL/IdTthL1, carrying the TthL1d1.4 gene (Tishchenko *et al*., 2007). The mutagenesis primers were 5′-TACGTGACCACCGTCATGGGCCCCAGCG-3′(sense) and 5′-GCTG GGGCCCATGACGGTGGT-3′ (antisense) and the flanking sequence primers XbaI-pET-fwd and HindIII-pET-rev (Tishchenko *et al*., 2007). The resulting final PCR product encoding Thr217Val TthL1d1 was cloned into the expression vector pET11a-PL. The nucleotide sequence of the cloned gene was verified by DNA sequencing.

Protein preparation and crystallization

Domain I of TthL1 with Thr217 replaced by valine was overproduced in *E.coli* strain BL21 (DE3) as a host. Purification of this mutant was performed as described for the isolated domain I of TthL1 (Tishchenko *et al*., 2007). After the final chromatography step, fractions containing the pure protein were pooled, dialysed into 30 mM Tris-HCl ($pH_{25°C}$ 7.5), 60 mM KCl and concentrated to 12 mg/ml using Vivaspin concentrators. The purification of MjaL1 (Köhrer *et al*., 1998) and of TthL1 (Nikonov *et al*., 1996) and of the mutant proteins Thr204Phe MjaL1 and Thr217Ala TthL1 (Nikonova *et al*., 2007) was described before.

Crystallization experiments were performed at 20°C by the hanging drop vapour diffusion method on siliconized glass cover slides in Linbro plates. Drops containing 2.5 µl of the protein solution at 12 mg/ml mixed with 1 µl of #17 of Crystal Screen Hampton Research precipitant solution (30% PEG 4000, 0.1 M Tris-HCl (pH25°C 8.5), 0.2 M $LiSO_4$,) and 1 µl of 15% (v/v) 2-methylpentane-2,4-diol (MPD) were equilibrated against 0.5 ml of the same precipitant solution. Protein crystals appeared after 2–3 days and grew to a maximum size of 0.35 mm × 0.1 mm × 0.05 mm within one week. Before freezing in liquid nitrogen, the crystals were transferred to the same precipitant solution.

Data collection and structure determination

Diffraction data were collected from a single crystal at EMBL beamline BW7A at DORIS storage ring, DESY (Hamburg, Germany) using a MAR CCD detector. Data were processed and merged with the XDS program suite (Kabsch, 2001). Crystals of Thr217Val TthL1d1 belong to space group $P3_1$ and diffract to 2.45 Å resolution. The cumulative intensity distribution calculated with DETWIN of the CCP4 program suite (Bailey, 1994) indicated hemihedral twinning. The twin fraction was estimated to be 0.45. The structure was solved by molecular replacement with PHASER (McCoy *et al*., 2005). The structure of unmodified TthL1d1 (PDB code 2OV7) was used as a search model.

The structure was refined with PHENIX (Adams *et al*., 2002) using target function for twinning refinement. The final model, refined to an R-factor of 19.6% and R-free of 25.3% at 2.45 Å resolution, includes 391 amino acids in three monomers and 40 water molecules. The quality of the model was checked with PROCHECK (Laskowski *et al*., 1993) and WHATCHECK (Hooft *et al*., 1996). Data and refinement statistics are summarized in Table 1.

Molecular dynamic simulations

The Molecular Dynamics (MDs) simulations for TthL1d1 and Thr217Val TthL1d1 have been performed with the GROMACS software (Lindahl *et al*., 2001) using optimized potentials for liquid simulations (OPLS) all atom force field (Jorgensen *et al*., 1996). LINCS algorithm (Hess *et al*., 1997) has been applied to constrain covalent bond lengths, allowing an integration time-step of 2 fs. Electrostatic interactions have been calculated using the Particle–Mesh Ewald method (Darden *et al*., 1993; Essmann *et al*., 1995) with a cut-off for Van der Waals interactions of 14 Å. The temperature has been kept constant (300 K) by separately coupling the protein and solvent to an external temperature bath ($\tau = 0.1$ ps) using Berendsen algorithm (Berendsen *et al*., 1984). The pressure has been kept constant (1 atm) by isotropic coupling to a pressure bath ($\tau = 0.5$ ps) using Parrinelo–Rahman algorithm (Bussi *et al*., 2007).

Table 1. Data collection and refinement statistics for Thr217Val TthL1d1

Data collection statistics[a,b]	
Space group	$P3_1$ (144)
Unit-cell parameters (Å, °)	$a = 77.7$, $b = 77.7$, $c = 48.1$ $\alpha = \beta = 90°$, $\gamma = 120°$
Wavelength (Å)	0.90
Resolution (Å)	15.0–2.45 (2.55–2.45)
Number of reflections	51588 (7424)
Number of unique reflections	10209 (1504)
Completeness (%)	96.2 (88.5)
Averaged redundancy	5.1 (4.9)
$I/\sigma_i(I)$[a]	12.4 (2.6)
R-merge (%)	9.6 (49.7)
Refinement statistics[a]	
Resolution range (Å)	20.0–2.45 (2.60–2.45)
Number of reflections	11819 (1850)
R-factor (%)	19.6 (28.2)
Free R-factor (%)	25.3 (32.0)
Twin operator	−k,−h,−l
Twin fraction	0.45
r.m.s. deviation	
Bond lengths (Å)	0.001
Bond angles (°)	0.4
Mean B value (overall, $Å^2$)	43.0

[a] Data collected at 110 K.
[b] Values in parenthesis are statistics for the highest resolution shell.

Journal of Molecular Recognition

The simulations have been started from the appropriate crystal structures. The proteins have been solvated in simple point charge (SPC) water molecules by adding a 15 Å layer of water around the protein in all three dimensions (about 25 000 water molecules). The total charge has been neutralized by Cl^- counter ions (from 3 to 15 depending on the total charge of the protein). For all the systems, a rectangular box has been used. After energy minimization and equilibration (during 50 ps), 1 ns trajectories have been calculated for each system. The coordinates have been saved at intervals of 1 ps.

SPR experiments

Real-time monitoring of the interactions between mutant L1 proteins and the 79-nt 23S rRNA fragment, containing the specific L1-binding site, was performed by SPR experiments (Katsamba *et al*., 2002) using the ProteOn XPR36 interaction array system (Bio-Rad, USA).

The specific 23S rRNA fragment of *M. vannielii* contains helixes 76 and 77, shortened helix 78, capped with tetraloop UUCG, and interconnecting loops A and B. This fragment was obtained by *in vitro* transcription with T7 RNA polymerase from linearized with *Sma*I plasmid pUC18, which carries the gene of specific 79-nt rRNA fragment. The rRNA fragment was purified by gel electrophoresis under denaturing conditions to a homogenous state. 5S rRNA from *Thermus thermophilus* isolated from cells (Nierhaus and Dohme, 1979) was used as a negative control.

The biotinylated 5S rRNA and rRNA fragment were prepared by ligating a short 3′-biotinylated RNA oligonucleotide to the corresponding RNA. The ligation mixture, containing 80 pmol of the rRNA fragment, 160 pmol of the 3′-biotinylated oligonucleotide, 3 μl of 10 × ligation buffer, 3 μl of 1 mM ATP, 3 μl of 10 mM hexamine cobalt chloride, 3 μl of BSA (10 mg/ml), 6 μl of 20% DMSO and 20 units of T4 RNA ligase (Fermentas) in a total volume of 30 μl, was incubated at 37°C for 4 h. Non-ligated oligonucleotides were removed by gel electrophoresis under denaturing conditions. The 3′-biotinylated rRNA probe was precipitated with ethanol, dissolved in Tris Mg Na (TMN buffer) (50 mM Tris–HCl, pH 7.5, 5 mM $MgCl_2$, 350 mM NaCl and 0.005% (v/v) BIAcore surfactant P20) and denaturated at 60°C for 2 min. The experiments were performed at 25°C. The biotinylated rRNA fragment was immobilized on a Neutravidin immobilized to polymer Layer with binding Capacity (ProteOn NLC sensor chip) at a constant concentration (500–600 RU) at a flow rate of 15 μl/min. The surface was then washed twice with 30 μl injections of regeneration solution (0.05% (w/v) Sodium Dodecyl Sulfate (SDS)) to remove RNA that was attached only loosely to the surface of the chip.

Five different concentrations of the analyte samples were prepared by serial dilution in TMN buffer for each set of sensorgrams. The samples were injected at a flow rate of 15 μl/min. The injection step included a 300–600 s association phase followed by a 1600–7200 s (20–120 min) dissociation phase in TMN buffer. All binding experiments were performed at 25°C. At the end of each cycle, the chip surface was regenerated by the injection of 30–150 μl of 0.1–0.2% SDS for the complete dissociation of proteins from the RNA probe. Response unit values were recorded at intervals of 0.9 s.

The sensorgrams were processed for baseline alignment and reference channel subtraction. In addition to the reference channel, interspot references were used for background subtraction. Kinetic analysis was performed by globally fitting curves describing a simple 1:1 bimolecular model to the set of five sensorgrams.

RESULTS

Earlier it was shown that domain I of ribosomal protein L1 is sufficient for specific RNA binding (Tishchenko *et al*., 2007). Domain I contacts RNA through the slightly concave surface formed by the inner face of the β-sheet, consisting of strands β1, β7, β8 and β9, and spatially adjacent loops α1–β1, β7–β8 and β9–β10 (Figure 1). *N*-terminal helix absent in archaeal L1 proteins contributes to the protein–RNA interactions in bacterial L1. Analysis of the crystal structures of the complexes formed by ribosomal protein L1 or its isolated domain I with 23S rRNA and mRNA fragments (Nikulin *et al*., 2003; Nevskaya *et al*., 2005, 2006; Tishchenko *et al*., 2008) shows that loop β9–β10 (Figure 1) containing the universally conserved triad Thr–Met–Gly plays very important role in RNA-binding. This triad comprising only 11% of all interacting residues is involved in 20% of RNA–protein contacts considered in the region up to 4.0 Å and about 40% of these contacts is formed by threonine. Such tight contact is suitable for studying the influence of a relief modification on the RNA-binding properties of the L1 protein. The hydroxyl and the main-chain carbonyl group of the threonine residue as well as the main-chain carbonyl group of the glycine residue form inaccessible hydrogen bonds with polar RNA atoms. Therefore, it was a reasonable assumption that changes in the surface relief in this region could dramatically affect the affinity of L1 for RNA. To reveal changes in the conformation of the loop and its surroundings, we solved the crystal structure of Thr217Val TthL1d1 and analysed it together with the earlier determined structures of two other mutants, Thr217Ala TthL1 and Thr204Phe MjaL1 (Nikonova *et al*., 2007).

Thr217Val mutant of TthL1d1

The isolated domain I of TthL1 interacts with 23S rRNA almost with the same affinity as the intact protein (Table 2). Our assumption was that replacement of Thr217 by Val in TthL1d1 should retain the relief of its RNA-binding site. In the complex of the mutant L1 with RNA, this substitution would result in the loss of an intermolecular hydrogen bond formed by atoms $O\gamma_1$ of Thr217 and O_2' of G33 (Nevskaya *et al*., 2006) which could be replaced by a C–H···O bond without an essential loss of RNA-binding ability.

However, mutant Thr217Val TthL1d1 showed a dramatic decrease in affinity for RNA (Table 2). The association rate constant decreased by approximately one order of magnitude,

Table 2. Kinetic parameters of complex formation between wild type or mutant ribosomal L1 proteins and a specific 79-nt 23S rRNA fragment. 5S rRNA was used as a negative control

Protein	k_{ass} ($M^{-1}s^{-1}$)	k_{diss} (s^{-1})	K_D (M)
		23S rRNA	
MjaL1	7.97×10^6	2.17×10^{-6}	2.72×10^{-13}
T204F MjaL1	6.21×10^6	3.08×10^{-4}	4.97×10^{-11}
TthL1d1	9.50×10^5	1.42×10^{-5}	1.49×10^{-11}
T217V TthL1d1	4.23×10^4	2.24×10^{-2}	5.28×10^{-7}
TthL1	4.02×10^5	6.38×10^{-6}	1.59×10^{-11}
T217A TthL1	2.06×10^4	3.15×10^{-4}	1.53×10^{-8}
		5S rRNA	
T217A TthL1	1.22×10^3	3.00×10^{-2}	2.59×10^{-5}

while the dissociation rate constant increased by almost three orders as compared to wild type TthL1d1. This drastic difference in affinity for RNA of the mutant disagrees with our hypothesis that the Thr217Val substitution should not change the surface relief in the contact region.

To reveal possible relief modifications in the contact region of Thr217Val TthL1d1, its crystal structure was determined at 2.45 Å resolution. In the wild type protein, the side chain of Thr217 forms a hydrogen bond with the main chain nitrogen atom of Thr40. Besides, mutual position of loop β9–β10, *N*-terminal helix and loop α1–β1 is strongly stabilized by a network of hydrogen bonds. Comparison of the contact regions in the wild type TthL1d1 and its mutant is shown in Figure 2. It turned out that replacement of the hydroxyl group of Thr217 by the methyl group of Val shifts loop β9–β10 from its position in the wild type protein in the direction of Met218 by about 1.0 Å, forming a bulge on the protein surface. In the mutant the side chain of Met218 pushes out the *N*-terminal helix, thus moving away the α1–β1 loop. As a result, the relative position of loops α1–β1 and β9–β10 is changed and two hydrogen bonds between them through Glu39 are broken. Residue Glu39 becomes accessible to the solvent and loop α1–β1 containing the universally conserved Phe37, which plays an important role in RNA-binding (Nevskaya *et al*., 2006), acquires an additional flexibility. The MD experiment confirms that the Thr217Val mutation increases the flexibility of the TthL1d1 contact region, including helix αl, loop α1–β1 and loop β9–β10 (Figure 3).

Docking of Thr217Val TthL1d1 to RNA gives rise to collisions between the protein and RNA in the regions of Met218 and the K^+ ion, which is present within the interface of the TthL1—RNA complexes (Nevskaya *et al*., 2006). The main chain carbonyl oxygen atom of Val217 changes its position compared to that of Thr217 and could form the hydrogen bond with the sugar—phosphate moiety of RNA instead of the base of G33 in the wild type complex. Besides, the increased flexibility of loop α1–β1 allows a displacement of Phe37 and a penetration of the water molecule in the inner cavity of the protein—RNA interface. It is a reasonable assumption that the structural changes of the mutant result in the extremely high dissociation rate constant (Table 2).

Thr217Ala mutant of TthL1

To create a cavity on the surface of the RNA-binding region, we replaced Thr217 in the intact TthL1 protein by Ala, for this purpose a usual substitution. SPR experiments showed a reduced RNA-binding ability of Thr217Ala TthL1 (Table 2). This mutant displays a 20-fold decrease of the apparent association and a 50-fold increase of dissociation rate constants. To understand the reasons for this difference in affinity for RNA, we analysed in detail the crystal structure of the Thr217Ala TthL1 mutant, which had

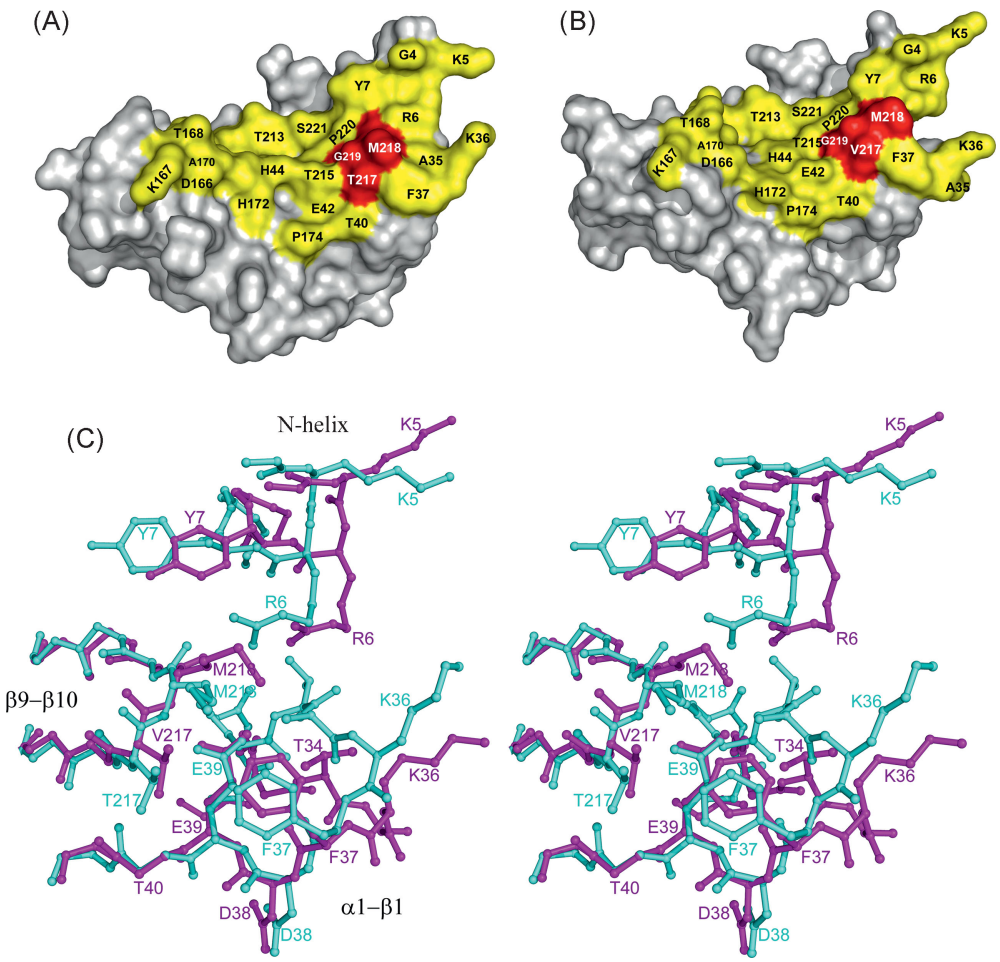

Figure 2. Comparison of the protein–RNA contact regions on the surfaces of the wild type TthL1d1 protein (A) and mutant Thr217Val TthL1d1 (B). Stereo view of Thr217Val TthL1d1 mutant superimposed onto corresponding region of the wild-type TthL1d1 (C). Mutation Thr217Val in TthL1d1 (magenta) changes relative position of *N*-terminal helix and loop α1–β1 as compared to that of wild type TthL1d1 (blue).

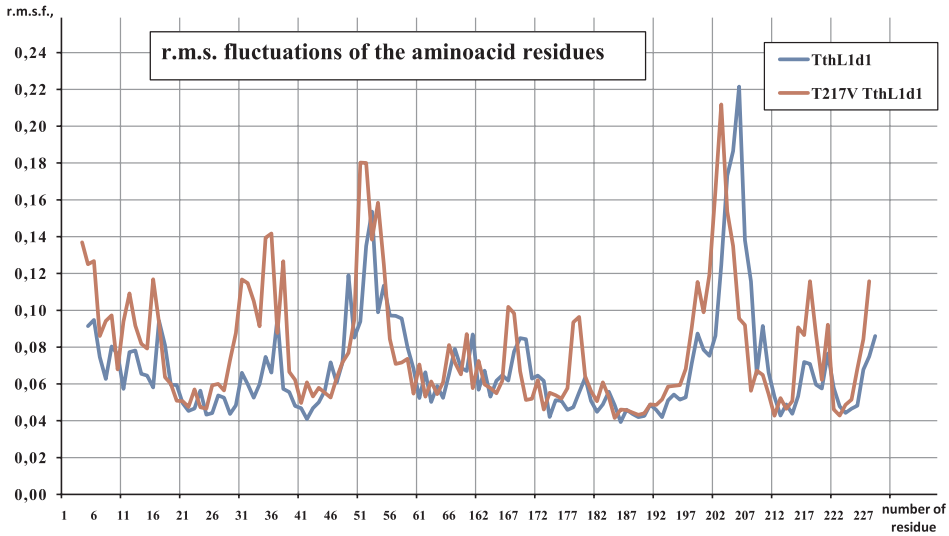

Figure 3. Root mean square fluctuations of the amino acid residues during MD-trajectories of Thr217Val TthL1d1.

been determined earlier in the unbound state (Nikonova *et al.*, 2007). Comparison of the mutant structure with that of the wild type TthL1 complexed with mRNA (Tishchenko *et al.*, 2007) showed that this mutation shifts the loop β9–β10 and produces a bulge on the molecular surface instead of the expected cavity. It was rather difficult to predict the resulting structural change beforehand as the position of this loop in the wild type protein is strongly stabilized by a network of hydrogen bonds. It is possible to suggest that only one of those H-bonds involving the Oγ_1 atom of Thr217 should be precluded by the Thr217Ala substitution. However, lack of two γ-atoms of threonine in the mutant protein provides a way for two water molecules to penetrate into the cavity between strands β1 and β9 (Figure 4). The water molecules induce changes in the RNA-binding region with the Cα atoms of Ala217 and Met218 shifted by approximately 1 and 2 Å, respectively, from their positions in the wild type protein. This results in displacement of loop β9–β10 and the formation of the bulge on the surface of the RNA-binding region. Moreover, each of the inserted water molecules forms the 'classical' network of four hydrogen bonds (Figure 4) and strongly stabilizes the modified conformation of the RNA-binding region. Docking of the mutant protein to the RNA molecule shows that the bulge on the RNA-binding surface prevents the formation of the network of hydrogen bonds, which stabilize the wild type L1—RNA complex. As a result, this mutant demonstrates a strongly decreased RNA-binding ability (Table 2).

Thr204Phe mutant of MjaL1

To create a bulge on the protein surface in the RNA-contact region, we replaced Thr204 in the triad Thr—Met—Gly of MjaL1 by phenylalanine. This mutation dramatically decreases the affinity of MjaL1 to 23S rRNA. SPR experiments show that the equilibrium dissociation constant (K_d) of the complex increased by almost two orders of magnitude compared to wild-type MjaL1. Only the apparent dissociation rate constant (k_{diss}) is responsible for this change, the mutation has no visible effect on the association rate constant (k_{ass}) (Table 2).

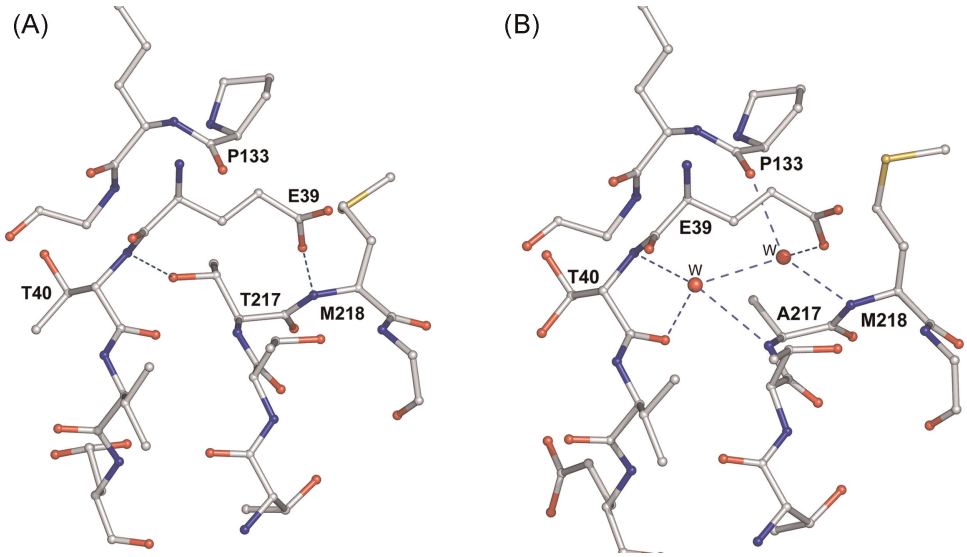

Figure 4. Hydrogen bonds formed by loop β9–β10 in the wild type TthL1 (A) and its Thr217Ala mutant (B).

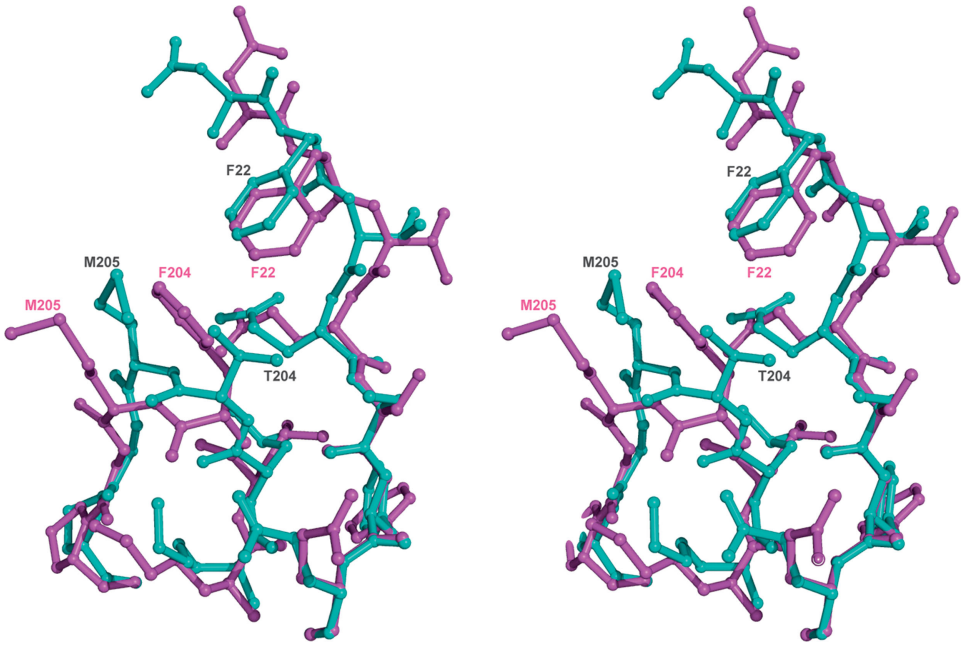

Figure 5. Comparison of the contact regions in the wild type (blue) and mutant MjaL1 proteins (magenta). Mutation Thr204Phe in MjaL1 produces a bulge on the protein surface stabilized by stacking interactions between Phe204, Met205 and Phe22.

To study structural changes in Thr204Phe MjaL1 contact region, we analysed the previously determined crystal structure of this mutant (Nikonova *et al.*, 2007) in context of its RNA-binding properties. The detailed analysis of the RNA-binding region of this mutant showed that the aromatic ring of Phe204 penetrates between Met205 and Phe22 (Figure 5) shifting the Met205 from its position in the wild type protein. Displacement of the Met205 Cα atoms is equal to 2.7 Å. Stacking interactions between side chains of all three residues (Phe204, Met205 and Phe22) stabilize the conformation of the modified RNA-binding region. Superposition of the structures of Thr204Phe MjaL1 and of MjaL1 in a complex with mRNA (Nevskaya *et al.*, 2005) shows that the side chain of Met205 of the mutant protein collides with the sugar−phosphate moiety of RNA. There is no possibility to avoid this collision using other Met rotamers. To prevent this collision, the protein has to be displaced from its position in the wild type L1−RNA complex by about 1.2 Å, or the RNA-binding region has to undergo a conformational change.

DISCUSSION

Allosteric effect of substitutions on the protein surface

Our analysis of the L1 mutant structures showed that substitutions on the protein surface, even what we considered as a neutral one such as Thr/Ala, induce conformational changes in regions next to the site of the mutation. These allosteric perturbations arise from the small shift of loop $\beta9$–$\beta10$ (not more than 1–2 Å) owing to a distortion of the intramolecular hydrogen bond between the main chain nitrogen atom of Thr40 and the hydroxyl group of Thr217. In all L1 mutants, investigated in this study, loops $\alpha1$–$\beta1$ and $\beta9$–$\beta10$ and helix $\alpha1$ changed their mutual positions so that the formation of the network of hydrogen bonds inherent to wild type L1−RNA complexes encountered serious obstacles.

Unexpectedly, the minimal displacements were found in the Thr204Phe MjaL1 mutant where only loop $\beta9$–$\beta10$ changed its conformation. The conformation of loop $\alpha1$–$\beta1$ was not altered and a small mutual shift of loops $\alpha1$–$\beta1$ and $\beta9$–$\beta10$ appeared, caused by the stacking interaction between Phe204, Met205 and Phe22. In the Thr217Ala and Thr217Val mutants, the disruption of the hydrogen bonds between loops $\beta9$–$\beta10$ and $\alpha2$–$\beta1$ through Glu39 resulted in the dramatic conformational changes of loop $\alpha1$–$\beta1$. In the Thr217Ala TthL1 mutant, additional hydrogen bonds between domain I and domain II were formed and stabilized the closed conformation of this protein. In accordance with our previous results (Tishchenko *et al.*, 2008), this decreased the association rate constant of the complex (Table 2). In the Thr217Val TthL1d1 mutant, the water molecules gained access to the interior of the protein−RNA interface due to conformational changes of loop $\alpha1$–$\beta1$. Besides, the substitution changed the mutual positions of loop $\beta9$–$\beta10$, strand $\beta1$ and helix $\alpha1$ (Figure 2A, B). These conformational changes dramatically increased the dissociation rate constant of the protein−rRNA complex formed by this mutant.

In this study we could show that replacement of a surface amino acid residue by residues, which are of the same size or even smaller, unexpectedly produced a bulge on the protein surface of the RNA-contact region, thus decreasing the affinity of the mutant for RNA. The formation of such bulges was found in all mutants analysed in this study. Worthy of note is the role of the solvent. Replacement of a large amino acid residue, such as threonine, by the small alanine allowed the water molecule to penetrate inward of the protein and to produce an unexpectedly stable conformation in the region of the mutation. This is a convincing example that solely the crystal structure of the mutant protein allows a correct analysis how the investigated mutation alters the affinity of the protein for RNA.

Influence of surface complementarity disruption on binding kinetics

All our attempts to obtain crystals of L1 mutants in complex with specific RNA fragments failed. Most likely, it is the result of an

Journal of Molecular Recognition

insufficient stability of the complexes since the analysis of kinetic parameters showed the strongly increased the dissociation rate constants. Apparently, L1 mutants and their RNA partners failed to induce the shape complementarity in the region of mutations due to the strongly stabilized bulges on the mutant surfaces. The highest increase of the dissociation rate constant was observed for the Thr217Val TthL1d1 mutant. Possibly, it is a result of the increased flexibility of the L1 contact regions adjacent to the triad, as MD experiments suggested.

The association rate constants were less drastically affected, they decreased approximately one order of magnitude. In the case of the Thr217Ala TthL1 mutant, the stabilization of the closed conformation could be responsible for maximum decrease of the association rate constant. TthL1 has to undergo a conformational change from the closed to the open conformation to bind RNA. Thus, the lower affinity could be mainly due to the impeded transition from the closed to the open conformation rather than to the altered relief of the protein surface.

To clarify whether the mutant L1 proteins recognize their specific target site on the 23S rRNA fragment, 5S rRNA was used as a negative control in the SPR experiments. Unfortunately, wild type MjaL1, TthL1 and TthL1d1 and the mutants, except Thr217Ala TthL1, aggregated at high concentrations required for our experiments with 5S rRNA. Only kinetic parameters of complex formation between Thr217Ala TthL1 and 5S rRNA could be measured (Figure 6). The apparent dissociation rate constant as well as the apparent equilibrium constant for the non-specific protein–RNA interactions differs dramatically compared to that for specific ones (Table 2). Therefore, it is clear that all L1 mutants studied specifically recognize their target RNA. Bulges created by amino acid substitutions on the protein surface in the RNA-binding region prevent the formation of the network of intermolecular hydrogen bonds inherent to the complexes formed by wild type protein L1 or its domain I. As a result, the mutant protein must be shifted or rotated relative to the RNA molecule, which in turn leads to a substantial increase of the dissociation rate constant and, correspondingly, to a decrease in life-time of the protein–RNA complex.

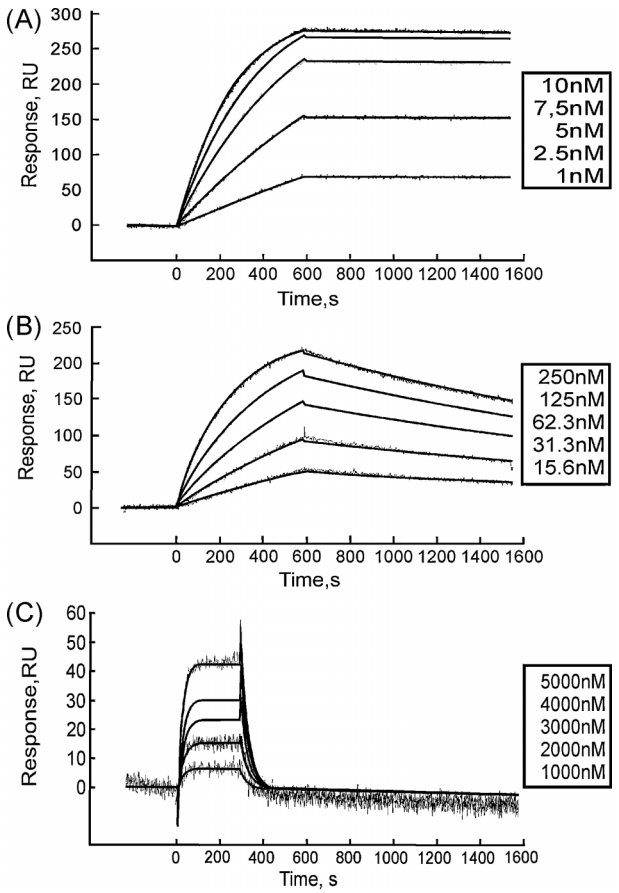

Figure 6. Sensorgrams showing kinetic analyses of the wild-type TthL1 (A) and mutant T217A TthL1 (B) with 79-nt fragment of 23S rRNA as well as interactions of mutant T217A TthL1 with 5S rRNA (C). Five analyte concentrations used for each dataset are shown. Association was monitored for 600 s with 79-nt fragment of 23S rRNA (A and B) and for 300 s with 5S rRNA (C). To obtain a high accuracy of the apparent dissociation rate constant (k_{diss}) for the wild-type protein the dissociation phase was increased from 1600 s for mutant (B and C) up to 7200 s for TthL1 (A). Bold lines represent the global fit of data sets using 1:1 models.

CONCLUSION

Site-directed mutagenesis can result in unexpected changes of the molecule structure. Therefore, a reliable interpretation of experimental results obtained for mutant proteins requires a preliminary determination of the spatial structure of studied mutants. Here we combined kinetic data of the mutant L1–rRNA complex formation with the structural analysis of the proteins with due regard for structural changes in the mutant protein. Our study shows that disruption of shape complementarity and appearance of 1–2 Å bulges in the protein–RNA contact region does not hinder specific recognition of the RNA target site but is crucial for the life-time of the protein–RNA complex.

Acknowledgements

This research was supported by the Russian Academy of Sciences, the Russian Foundation for Basic Research (grant #10-04-00618-a), the Program of RAS on Molecular and Cellular Biology, the Program of the RF President on support of outstanding scientific schools and the Austrian Science Fund (FWF, P17164-B10 to W.P.). The research of M.G. was supported in part by International Research Scholar's award from the Howard Hughes Medical Institute, that of O.K. by fellowships from EMBO (ASTF 113-2008) and FEBS.

REFERENCES

Adams PD, Grosse-Kunstleve RW, Hung L-W, Ioerger TR, McCoy AJ, Moriarty NW, Read RJ, Sacchettini JC, Sauter NK, Terwilliger TC. 2002. PHENIX: building new software for automated crystallographic structure determination. *Acta Crystallogr.* **D58**: 1948–1954.

Bailey S. 1994. The CCP4 suit: programs for protein crystallography. *Acta Crystallogr.* **D50**: 760–763.

Berendsen HJC, Postma JPM, DiNola A, Haak JR. 1984. Molecular dynamics with coupling to an external bath. *J. Chem. Phys.* **81**: 3684–3690.

Bussi G, Donadio D, Parrinello M. 2007. Canonical sampling through velocity rescaling. *J. Chem. Phys.* **126**: 014101.

Darden T, York D, Pedersen L. 1993. Particle mesh Ewald: an N_log(N) method for Ewald sums in large systems. *J. Chem. Phys.* **98**: 10089–10092.

Essmann U, Perera L, Berkowitz ML, Darden T, Lee H, Pedersen LG. 1995. A smooth particle mesh Ewald method. *J. Chem. Phys.* **103**: 8577–8593.

Hanner M, Mayer C, Köhrer C, Golderer G, Gröbner P, Piendl W. 1994. Autogenous translational regulation of the ribosomal MvaL1 operon

in the archaebacterium *Methanococcus vannielii*. *J. Bacteriol.* **176**: 409–418.
Hess B, Bekker H, Berendsen HJC, Fraaije JEM. 1997. LINCS: a linear constraint solver for molecular simulations. *J. Comput. Chem.* **18**: 1463–1472.
Ho SN, Hunt HD, Horton RM, Pullen JK, Pease LR. 1989. Site-directed mutagenesis by overlap extension using the polymerase chain reaction. *Gene* **77**: 51–59.
Hooft RWW, Vriend G, Sander C, Abola EE. 1996. Errors in protein structures. *Nature* **381**: 272–272.
Jorgensen WL, Maxwell DS, Tirado-Rives J. 1996. Development and testing of the OPLS all-atom force field on conformational energetic and properties of organic liquids. *J. Am. Chem. Soc.* **118**: 11225–11236.
Kabsch W. 2001. Integration, scaling, space-group assignment and post refinement. XDS. In International Tables for Crystallography, vol. F, Rossmann MG, Arnold E (eds). Kluwer Academic Publishers: Dordrecht.
Katsamba PS, Park S, Laird-Offringa IA. 2002. Kinetic studies of RNA-protein interactions using surface plasmon resonance. *Methods* **26**: 95–104.
Köhrer C, Mayer C, Neumair O, Gröbner P, Piendl W. 1998. Interaction of ribosomal L1 proteins from mesophilic and thermophilic Archaea and Bacteria with specific L1-binding sites on 23S rRNA and mRNA. *Eur. J. Biochem.* **256**: 97–105.
Laskowski RA, MacArthur MW, Moss DS, Thornton JM. 1993. PROCHECK: a program to check the stereochemical quality of protein structures. *J. Appl. Crystallogr.* **26**: 283–291.
Lindahl E, Hess B, Van der Spoel D. 2001. GROMACS 3.0: a package for molecular simulation and trajectory analysis. *J. Mol. Model.* **7**: 306–317.
McCoy AJ, Grosse-Kunstleve RW, Storoni LC, Read RJ. 2005. Likelihood-enhanced fast translation functions. *Acta Crystallogr.* **D61**: 458–464.
Nevskaya N, Tishchenko S, Fedorov R, Al-Karadaghi S, Lilyas A, Kraft A, Piendl W, Garber M, Nikonov S. 2000. Archaeal ribosomal protein L1: the structure provides new insights into RNA binding of the L1 protein family. *Structure* **8**: 363–371.
Nevskaya N, Tishchenko S, Gabdoulkhakov A, Nikonova E, Nikonov O, Nikulin A, Platonova O, Garber M, Nikonov S, Piendl W. 2005. Ribosomal protein L1 recognizes the same specific structural motif in its target sites on the autoregulatory mRNA and 23S rRNA. *Nucleic Acids Res.* **33**: 478–485.
Nevskaya N, Tishchenko S, Paveliev M, Smolinskaya Yu, Fedorov R, Piendl W, Nakamura Y, Toyoda T, Garber M, Nikonov S. 2002. Structure of ribosomal protein L1 from *Methanococcus thermolithotrophicus*. Functionally important structural invariants on the L1 surface. *Acta Crystallogr.* **D58**: 1023–1029.
Nevskaya N, Tishchenko S, Volchkov S, Kljashtorny V, Nikonova E, Nikonov O, Nikulin A, Köhrer C, Piendl W, Zimmermann R, Stockley P, Garber M, Nikonov S. 2006. New insights into interaction of ribosomal protein L1 with RNA. *J. Mol. Biol.* **355**: 747–759.
Nierhaus KH, Dohme F. 1979. Total reconstitution of 50S subunits from *Escherichia coli* ribosomes. *Meth. Enzymol.* **59**: 443–449.
Nikonov S, Nevskaya N, Eliseikina I, Fomenkova N, Nikulin A, Ossina N, Garber M, Jonsson B-H, Briand C, Svensson A, Aevarsson A, Liljas A. 1996. Crystal structure of the RNA-binding ribosomal protein L1 from *Thermus thermophilus*. *EMBO J.* **15**: 1350–1359.
Nikonova E, Volchkov S, Kljashtorny V, Tishchenko S, Kostareva O, Nevskaya N, Nikonov O, Gabdoulkhakov A, Nikulin A, Davydova N, Streltsov V, Garber M, Nikonov S. 2007. Crystal structures of mutant ribosomal proteins L1. *Mol. Boil. (Mosk.)* **41**: 688–696.
Nikulin A, Eliseikina I, Tishchenko S, Nevskaya N, Davydova N, Platonova O, Piendl W, Selmer M, Liljas A, Drygin D, Zimmermann R, Garber M, Nikonov S. 2003. Structure of the L1 protuberance in the ribosome. *Nat. Struct. Biol.* **10**: 104–108.
Tishchenko S, Kljashtorny V, Kostareva O, Nevskaya N, Nikulin A, Gulak P, Piendl W, Garber M, Nikonov S. 2008. Domain II of *Thermus thermophilus* ribosomal protein L1 hinders recognition of its mRNA. *J. Mol. Biol.* **383**: 301–305.
Tishchenko S, Nikonova E, Kljashtorny V, Kostareva O, Nevskaya N, Piendl W, Davydova N, Streltsov V, Garber M, Nikonov S. 2007. Domain I of ribosomal protein L1 is sufficient for specific RNA binding. *Nucleic Acids Res.* **35**: 7389–7395.
Tishchenko S, Nikonova E, Nikulun A, Nevskaya N, Volchkov S, Piendl W, Garber M, Nikonov S. 2006. Structure of ribosomal protein L1-mRNA complex at 2.1 Å resolution. Common features of crystal packing of L1-RNA complexes. *Acta crystallogr.* **D62**: 1545–1554.